frontiers | Frontiers in Earth Science

TYPE Original Research
PUBLISHED 09 September 2022
DOI 10.3389/feart.2022.966558

OPEN ACCESS

EDITED BY
Wenjun Zheng,
Sun Yat-sen University, China

REVIEWED BY
Chuanyong Wu,
Institute of Disaster Prevention, China
Haibo Yang,
China Earthquake Administration, China
Yiquan Li,
Nanjing University, China

*CORRESPONDENCE
Mingjian Liang,
23800794@qq.com

SPECIALTY SECTION
This article was submitted to Structural Geology and Tectonics, a section of the journal Frontiers in Earth Science

RECEIVED 11 June 2022
ACCEPTED 19 August 2022
PUBLISHED 09 September 2022

CITATION
Zuo H, Qin Y, Liang M, Sun K, Huang F, Liao C, Zhou W, Wu W, Zhang H and Yang Y (2022), Geological and geomorphological evidence of holocene activity along the maisu fault in the northern Sichuan–Yunnan block, Tibetan Plateau.
Front. Earth Sci. 10:966558.
doi: 10.3389/feart.2022.966558

Geological and geomorphological evidence of holocene activity along the maisu fault in the northern Sichuan–Yunnan block, Tibetan Plateau

Hong Zuo[1,2], Yulong Qin[3], Mingjian Liang[1,2]*, Kai Sun[4], Feipeng Huang[4], Cheng Liao[1,2], Wenying Zhou[1,2], Weiwei Wu[1,2], Huiping Zhang[4,5] and Yao Yang[1]

[1]Sichuan Earthquake Agency, Chengdu, China, [2]Chengdu Institute of Tibetan Plateau Earthquake Research, China Earthquake Administration, Chengdu, China, [3]Sichuan Geological Survey, Chengdu, China, [4]State Key Laboratory of Earthquake Dynamics, Institute of Geology, China Earthquake Administration, Beijing, China, [5]Lhasa National Geophysical Observation and Research Station, Institute of Geology, China Earthquake Administration, Lhasa, China

The Sichuan–Yunnan block is located in the eastern of Tibetan Plateau and exhibits strong tectonic and earthquake activity. The Maisu fault is an E–W-trending fault within this block. Via interpretations of remote-sensing imagery and field surveys, we identified a earthquake surface rupture zone that has developed along the Maisu fault; we then estimated its Holocene activity. The surface rupture extends westward from the town of Puma, Sichuan Province, to the village of Worilong, Xizang Province, and has a length of approximately 45 km. According to a fault outcrop and carbon-14 dating of a profile near the village of Yongqu, Xizang Province, the most recent earthquake along this rupture may have occurred after 1850 ± 30 BP. The Maisu fault extends eastward and may intersect the Garzê–Yushu fault. Accordingly, as a secondary fault, the Maisu fault likely accommodates the partitioned horizontal slip deformation of the Garzê–Yushu fault.

KEYWORDS

Maisu fault, Garzê–Yushu fault, Holocene activity, surface rupture, Sichuan–Yunnan block

1 Introduction

The Sichuan–Yunnan block in the eastern Tibetan Plateau is located in a region of China that has strong tectonic and earthquake activity (Deng et al., 2014; Yuan et al., 2020). In the eastern margin of the plateau, several strong and major earthquakes (i.e., the 2008 Mw7.9 Wenchuan, 2010 Mw6.9 Yushu, 2013 Mw6.6 Lushan, and 2017 Mw6.5 Jiuzhaigou earthquakes) have occurred over the past 2 decades (Xu et al.,

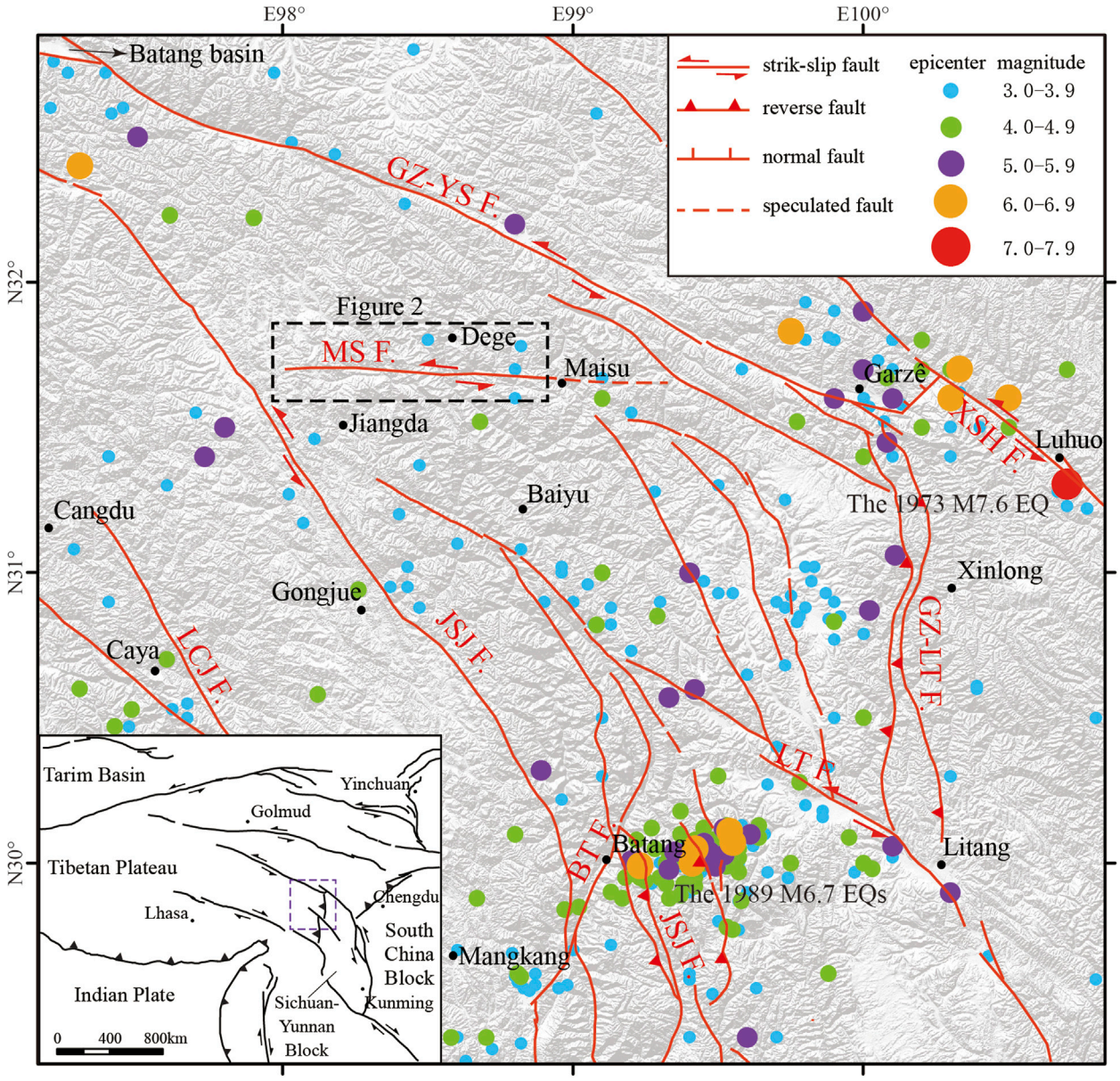

FIGURE 1
Distribution of the main faults and strong earthquakes within the study region. GZ-YS F, The Garzê–Yushu fault; XSH F, The Xianshuihe fault; GZ-LT F, The Garzê–Litang fault; MS F, The Maisu fault; LT F, The Litang fault; JSJ F, The Jinshajiang fault; BT F, The Batang fault; and LCJ F, The Lancangjiang fault.

2008; Wen et al., 2009; Lin et al., 2011; Zhou et al., 2014; Yi et al., 2017). The occurrence of these strong earthquakes is closely related to active faults along the eastern margin of the Tibetan Plateau, and the Garzê–Yushu fault is one such left-lateral strike-slip fault associated with major earthquake activity. The Garzê–Yushu fault and the Xianshuihe fault form a left-stepping pattern and together constitute the northern boundary of the Sichuan–Yunnan block (Zhou et al., 1996; Wen et al., 2003; Xu et al., 2003; Zhao et al., 2021). From the southeast to the northwest, the Garzê–Yushu fault can be divided into five segments: the Garzê, Manigange, Dengke, Yushu, and Dangjiang segments. Major earthquakes have occurred along these fault segments, e.g., the 1866 M7.5 earthquake on the Garzê segment, the 1896 M7.3 earthquake on the Dengke segment, the Yushu M7.1 earthquake on the Yushu segment, and the 1738 M > 7 earthquake on the Dangjiang segment (Wen et al., 2003; Lü, 2017).

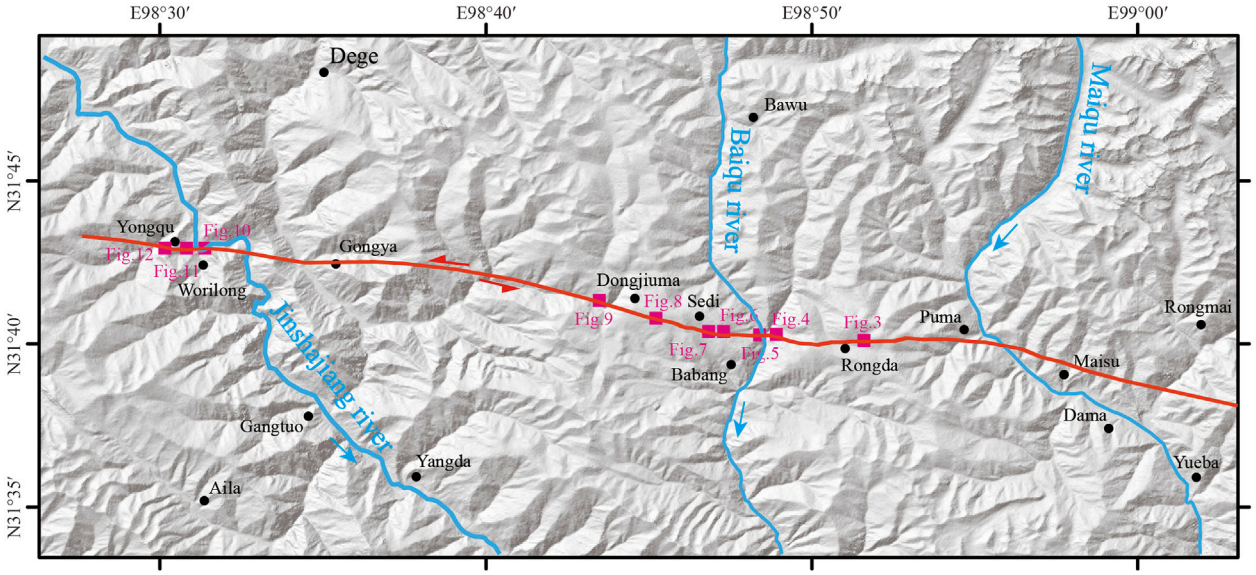

FIGURE 2
Tracks showing Holocene activity along the Maisu fault. Locations of studied sites are shown.

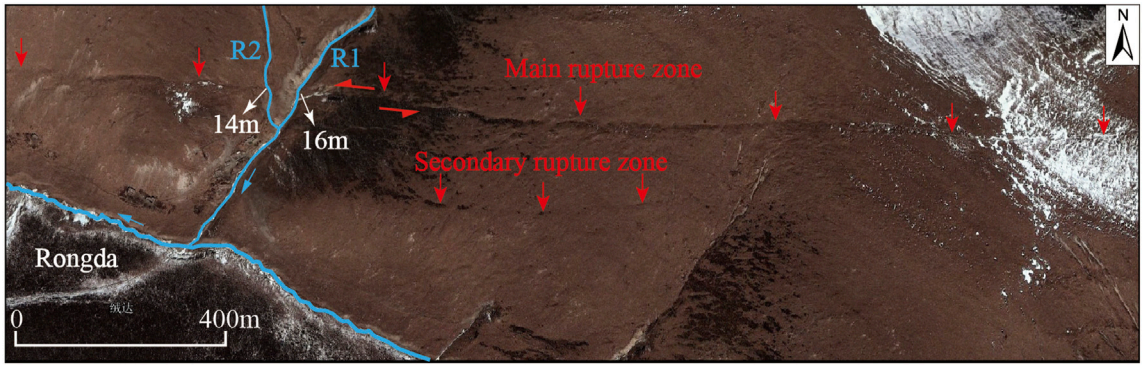

FIGURE 3
Surface rupture on the Maisu fault near Rongda, west of Puma. The image was obtained from Google Earth (reference coordinates: E98.85883°, N31.66850°).

There are also several E–W-trending faults on the southern side of the Garzê–Yushu fault, such as the southern boundary fault of the Batang Basin. This fault, which intersects the Garzê–Yushu fault at an angle of 30°, not only exhibits Holocene activity but also accommodates the horizontal slip rate of the Garzê–Yushu fault (Huang et al., 2015; Lü, 2017). South of Dege County, there is another E–W-trending fault called the Maisu fault, which cuts the Triassic and Tertiary strata forming a linear negative topography. The Maisu fault is a left-lateral strike-slip fault that was thought to be a late-Pleistocene-active fault (Xu et al., 2016). Our field study, however, indicates that the Maisu fault is a Holocene-active fault. This finding has important implications for our understanding of the tectonic deformation and regional strain partitioning of the Sichuan–Yunnan block. Furthermore, it is useful to study the characteristics of the regional strong earthquake activity in this block. In this article, on the basis of high-resolution satellite imagery and detailed fieldwork, we map the surficial track of the Maisu fault and present geological and geomorphological evidence of its Holocene activity.

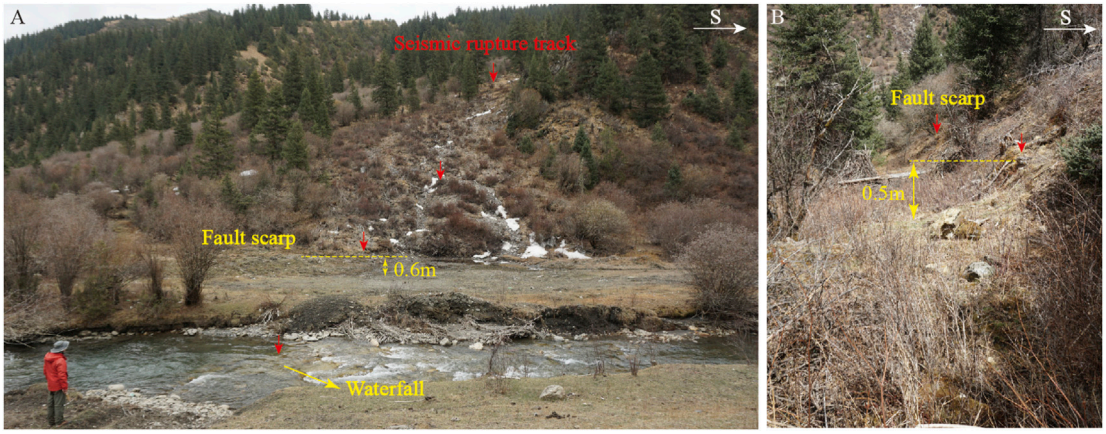

FIGURE 4
Seismic surface rupture zone near the Baiqu River northeast of Babang. **(A)** Seismic scarp and waterfall developed along the surface rupture zone (E98.80997°, N31.67147°), and **(B)** seismic scarp with a height of 0.5 m (E98.80790°, N31.67189°).

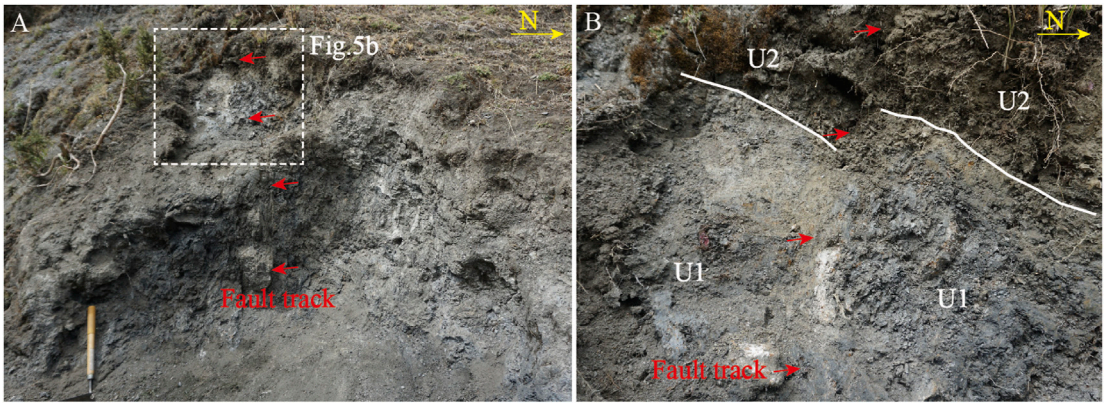

FIGURE 5
Fault outcrop on a hillside along the Baiqu River near Babang (E98.80776°, N31.67190°). **(A)** Photograph showing that the fault has dislocated all of the stratigraphic units in the outcrop profile, and **(B)** close-up photograph of unit U2, which was dislocated by the fault.

2 Tectonic setting

The study area is located in the northwestern margin of the Sichuan–Yunnan block. It lies between the Jinshajiang suture and the Garzê–Litang suture but is closer to the former. The Jinshajiang suture experienced the Indosinian subduction–collision orogeny and the late Yanshanian–Himalayan strike-slip transition (Hou et al., 1995; Wu et al., 2014; Zeng and Xu, 2019; Xia and Zhu, 2020). Within the study region, there are NW–SE-trending, NNE–SSW-trending, E–W-trending, and S–N-trending fault systems controlled by the Jinshajiang, Garzê–Litang, and Garzê–Yushu fault zones. The S–N-trending Jinshajiang fault zone was produced by the closure of the Tethys Ocean. This complex fault zone has a width of approximately 50 km from east to west and comprises five main faults (Xu et al., 1992; Zhou et al., 2005). The southern segment of the Jinshajiang fault zone exhibits Holocene fault activity (Zhou et al., 2005; Xia and Zhu, 2020). Many M6.0–6.9 earthquakes have been documented as occurring along this segment (Zhou et al., 2005; Wu et al., 2019). Its northern segment also exhibits late Quaternary activity (Wu et al., 2019); however, no historical records of strong earthquakes exist. To the south, the NE–SW-trending Batang fault intersects with the Jinshajiang fault zone at an acute angle, showing obvious Holocene dextral strike-slip fault activity; in addition, the 1870 M7.3 earthquake occurred on this fault (Zhou et al., 2005). The NW–SE-trending Litang fault is located on the northeastern side of the Jinshajiang fault, showing left-lateral strike-slip fault activity during the Holocene (Xu et al., 2005;

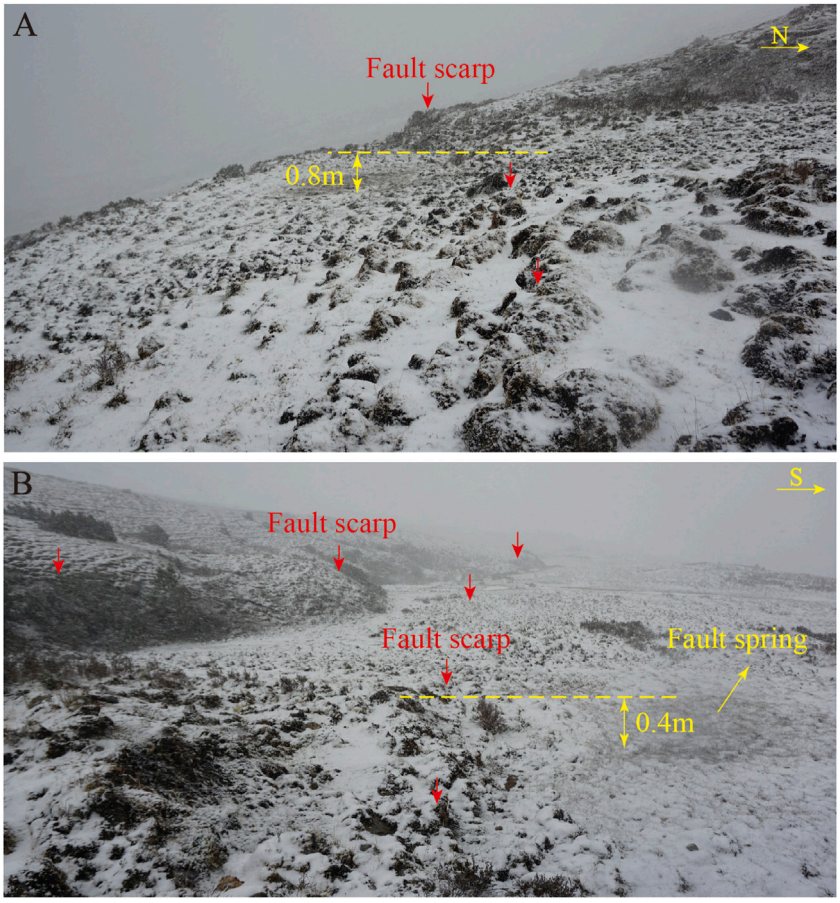

FIGURE 6
Track of the seismic surface rupture near the village of Sedi, close to Babang. **(A)** Seismic scarp developed on the alluvial fan (E98.78315°, N31.67171°), and **(B)** fault and seismic scarp developed on the alluvial fan, with a fault spring developed under the scarp (E98.78173°, N31.67198°).

Zhou et al., 2005; Chevalier et al., 2016). This fault controlled the formation and evolution of Tertiary–Quaternary basins such as the Maoyaba, Litang, and Jiawa basins. The Litang fault also produced the 1948 M7.3 and 1890 M > 7 earthquakes (Xu et al., 2005; Zhou et al., 2005; Chevalier et al., 2016). The Garzê–Yushu fault constitutes the northern boundary of the Sichuan–Yunnan block. It is a Holocene-active sinistral strike-slip fault, and its horizontal slip rate is estimated to have been 5–12 mm/a in the late Quaternary (Zhou et al., 1996, 1997; Wen et al., 2003; Peng et al., 2006; Chevalier et al., 2017). Earthquakes with magnitudes of M7.3 (1986), M7.7 (1854), M7.3 (1896), M7.1 (2010), and M > 7 (1738) have occurred along the Garzê–Yushu fault (Wen et al., 2003; Lin et al., 2011; Li et al., 2016; Lü, 2017). The Maisu fault is located to the south of the Garzê–Yushu fault, and its eastward extension may intersect the Garzê–Yushu fault. These active faults constitute the tectonic framework of the study area and control the regional tectonic deformation.

The current fault activity within the study area is unevenly distributed. Specifically, the distribution of destructive earthquakes is controlled by the active faults. Recent major earthquakes have concentrated primarily along the Xianshuihe fault and in the Jinshajiang fault zone (Figure 1). For example, the Luhuo M7.6 earthquake in 1973 occurred on the Xianshuihe fault and the M6.7 earthquake in 1989 occurred in the northern section of the Jinshajiang fault zone. However, current fault activity in other areas, dominated by small earthquakes with magnitudes of ≤M5, is more scattered.

3 Materials and methods

In this study, we used high-resolution satellite images (Google Earth) and 30-m-resolution Shuttle Radar Topography Mission data to estimate the track of late Quaternary activity along the Maisu fault. On the basis of interpretations of these data and tectonic geomorphological survey data, we determined the fault track of the Maisu fault using geomorphological markers such as fault scarps, deflected stream channels and terraces, and linear fault valleys.

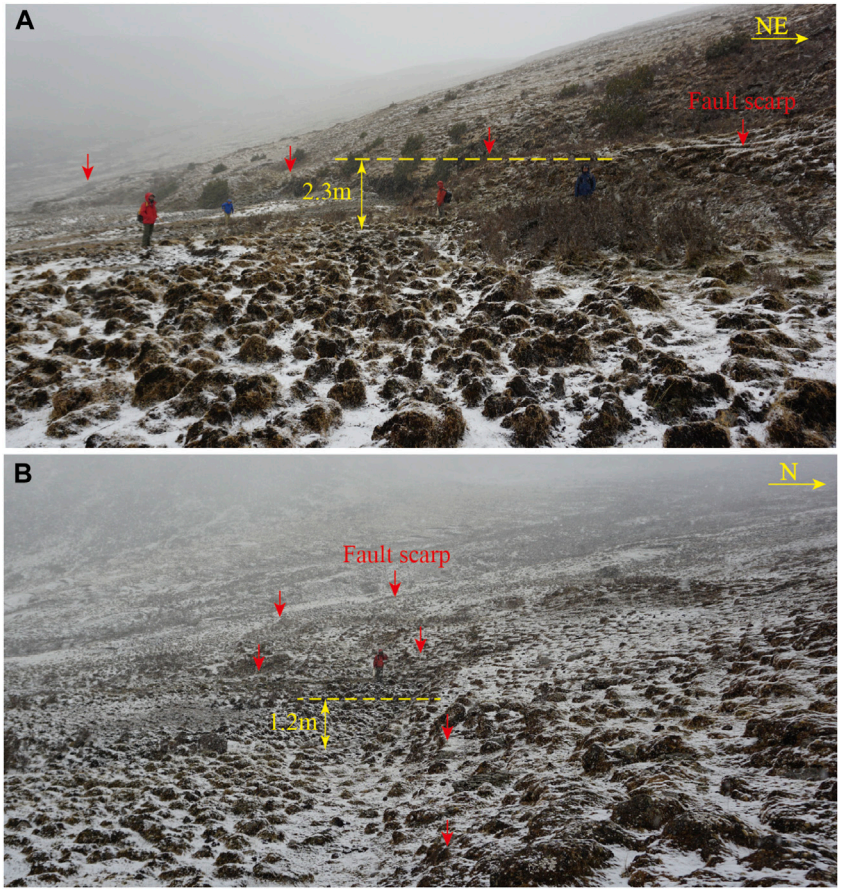

FIGURE 7
Track of the seismic surface rupture near Sedi, close to Babang. **(A)** Linear fault scarp and seismic scarp (E98.78100°, N31.67214°), and **(B)** partial segment rupture zone where the zone diverges into multiple branches (E98.77832°, N31.67261°).

In our field survey, unmanned aerial vehicle technology was used to obtain high-resolution geomorphological images. Using the ESRI ArcMap software, we generated digital images of the tectonic deformation. Via an analysis of these images and the field survey data, we examined the evolution of the deformed landforms and their cumulative displacement as a result of fault motion. Furthermore, a geological outcrop and the carbon-14 dating method allowed us to identify Holocene activity along the Maisu fault. The carbon-14 samples were analyzed at a laboratory operated by Beta Analytic Inc. United States. On the basis of the geomorphological markers and the radiocarbon dating of the strata displaced by the fault in the geological outcrop, we estimated the Holocene activity of the Maisu fault. Finally, we used formulas suggested by Wells and Coppersmith (1994) to calculate the magnitude of the latest strong earthquake that occurred along the Maisu fault.

4 Results

An analysis of the remote-sensing and field survey data revealed Holocene activity along the Maisu fault, as well as well-preserved surface ruptures. The Jinshajiang River and its main tributaries, such as the Baiqu and Maiqu rivers, pass through the Maisu fault and are obviously left-laterally displaced by the fault (Figure 2). Furthermore, the surface rupture zone on the fault extends from the town of Puma to north of the towns of Babang and Gongya in Dege County, Sichuan Province, and then finally disappears near the village of Worilong, near the town of Gangtuo, Xizang Province. The fault has a length of approximately 45 km (Figure 2). From east to west, some representative sites are described as following.

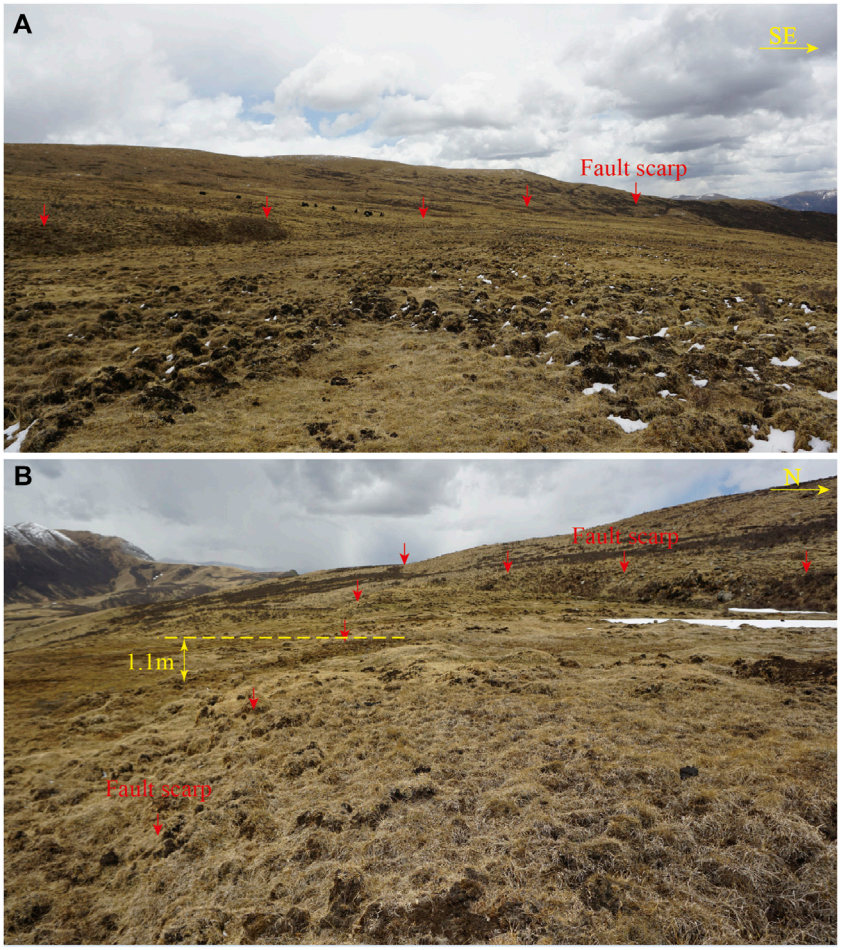

FIGURE 8
Seismic surface rupture track near Dongjiuma, close to Babang. **(A)** Fault scarp developed on the piedmont alluvial fan (E98.75844°, N31.67840°), and **(B)** seismic scarp developed in front of the older fault scarp (E98.75308°, N31.679,021°).

4.1 The rongda site

In Rongda, west of Puma, many geomorphological markers of recent Maisu fault activity are well preserved; for example, there exists a well-defined linear track of the recent fault activity, fault scarps, and gullies that are left-laterally displaced by 16 m (Gully R1) and 14 m (Gully R2) (Figure 3). This segment is close to the eastern end of the rupture zone, where it spreads out into multiple secondary rupture tracks (Figure 3).

4.2 The babang site

Approximately 3.2 km northeast of Babang, the surface rupture has formed a shallow linear trough on the hillside on the eastern bank of the Baiqu River; in addition, it has formed a fault scarp with a height of 0.6 m on terrace T1 and a waterfall on the Baiqu River (Figure 4A). There is a linear fault scarp with a height of approximately 0.5 m on another hillside along the Baiqu River (Figure 4B). Moreover, a natural fault outcrop is exposed, revealing that the fault displaced the top alluvial gravel and sand layer (Figure 5A). As shown in Figure 5B, unit U1 is composed of dark gray silt and gravel, representing a sag pond deposit facies. Unit U2 is composed of brown sand and gravel, representing a diluvial deposit facies. The fault orientation is approximately 280°, and the fault is steeply dipping. The fault displaced unit U2 upward to the ground surface and formed the surface rupture, likely reflecting the most recent major earthquake (Figure 5B).

4.3 The sedi site

At the Sedi site (approximately 3.0 km northwest of Babang), the earthquake surface rupture is also obvious. The rupture zone

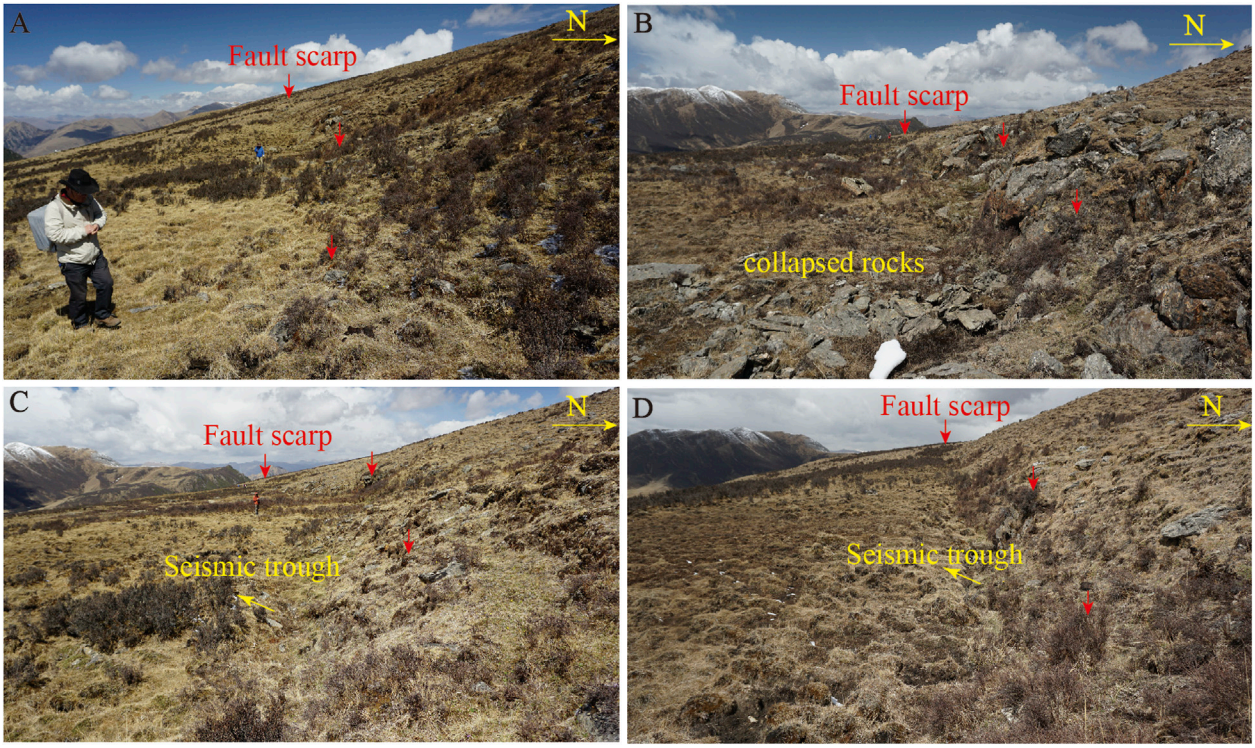

FIGURE 9
Seismic surface rupture track near Dongjiuma, close to Babang. **(A)** Seismic scarp (E98.74541°, N31.68088°), **(B)** seismic scarp and collapsed rocks under the scarp as a result of an earthquake (E98.74636°, N31.68085°), and **(C)** and **(D)** seismic troughs developed under the scarp as a result of an earthquake (coordinates E98.74887°, N31.6807° and E98.75156°, N31.67963°, respectively).

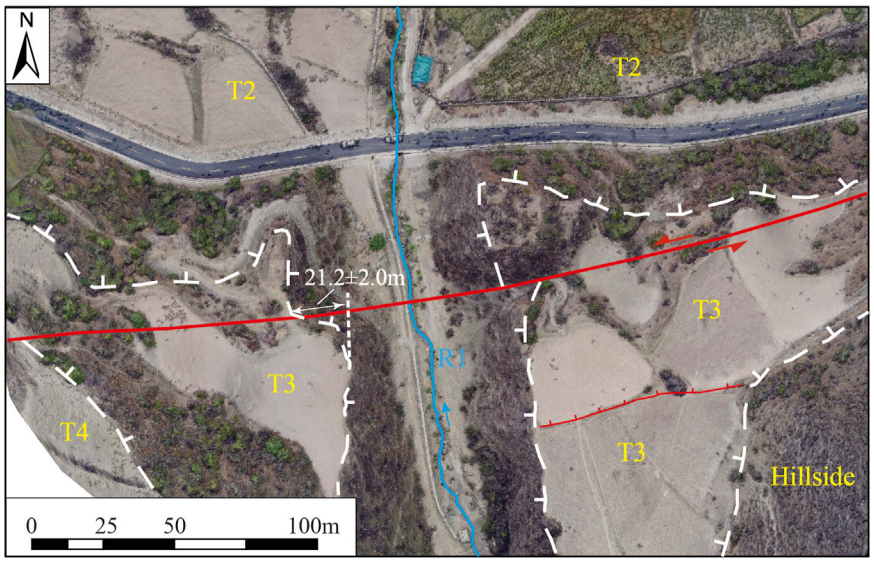

FIGURE 10
Terrace (T3) of the Jinshajiang River left-laterally displaced by the Maisu fault, near Worilong, close to Gangtuo, Xizang Province (E98.51997°, N31.71514°). The image was acquired using unmanned aerial vehicle photogrammetry. The white dashed lines represent the terrace riser. R1 is a tributary of the Jinshajiang river.

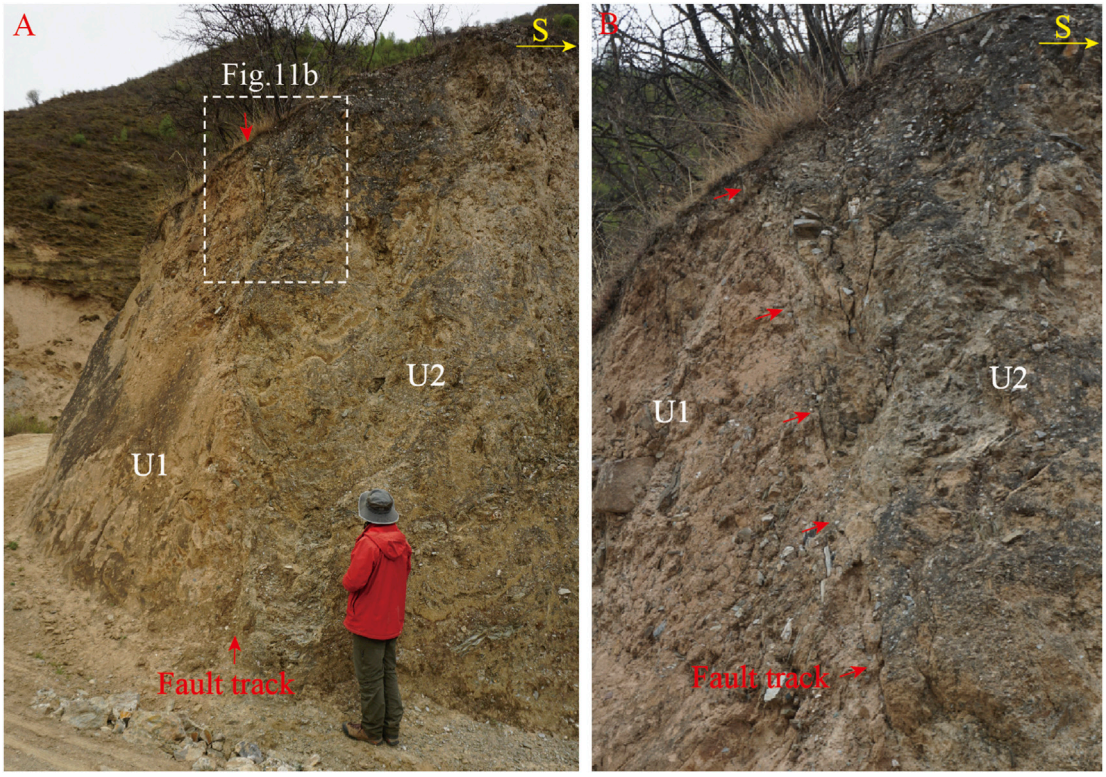

FIGURE 11
Fault outcrop of the Maisu fault near Yongqu, close to Gangtuo (E98.51560°, N31.71525°). **(A)** Photograph showing the fault outcrop, unit U1 is composed of alluvial sand–gravel, and unit U2 is composed of tectonic breccia and clastic rock from the fault zone. **(B)** Close-up photograph of the area shown by the dashed rectangle in panel A.

developed along the older fault scarp or formed a new fault scarp on the alluvial fan in the front of the older scarp. As shown in Figure 6A, the surface rupture zone developed on the latest alluvial fan with a scarp height of approximately 0.8 m, while the older fault scarp was heavily degraded (Figure 6A). Figure 6B shows that the surface rupture developed nearly parallel to the older fault scarp, forming a fault scarp with a height of 0.3–0.6 m (Figure 6B), and a fault spring was exposed on the front of the new scarp. The surface rupture also developed on top of the older fault scarp (Figure 7A) or the partial segment rupture zone diverged into multiple branches (Figure 7B).

4.4 The dongjiuma site

Just east of the village of Dongjiuma, the Maisu fault cuts through the piedmont alluvial fan, where it forms a linear fault scarp with a height of 1.5–3.0 m. The surface rupture developed along the bottom edge of the older scarp (Figure 8A) or cut through the newest alluvial fan in front of the older scarp to form a new fault scarp (Figure 8B). Extending to Dongjiuma, the fault cuts through the hillside, where a fault scarp has developed, as shown in Figure 9A. The field survey revealed collapsed debris in front of some segments of the older scarps (Figure 9B) or a seismic trough under the fault scarp (Figures 9C,D).

4.5 The worilong site

The Maisu fault extends westward, cuts across the Jinshajiang River just south of Gongya, and then enters the Xizang Province. The surface rupture zone extends to Gangtuo and then gradually disappears. At the Worilong site (northwest of Gangtuo), the Maisu fault cuts through terrace T3 of the Jinshajiang River; the terrace has been left-laterally displaced by 21.2 ± 2.0 m (Figure 10). Furthermore, multiple fault scarps are developed on the terrace. We identified a fault outcrop exposed on the southern side of a road near the village of Yongqu, close to Gangtuo. The fault profile revealed two main units (Figure 11A). Unit U1 consists of Quaternary strata and is composed of sand and gravel, representing a diluvial deposit facies (Figure 11B). Unit U2 is composed of tectonic breccia and clastic rock from the fault zone. The fault has displaced these two strata up to the ground surface (Figure 11B).

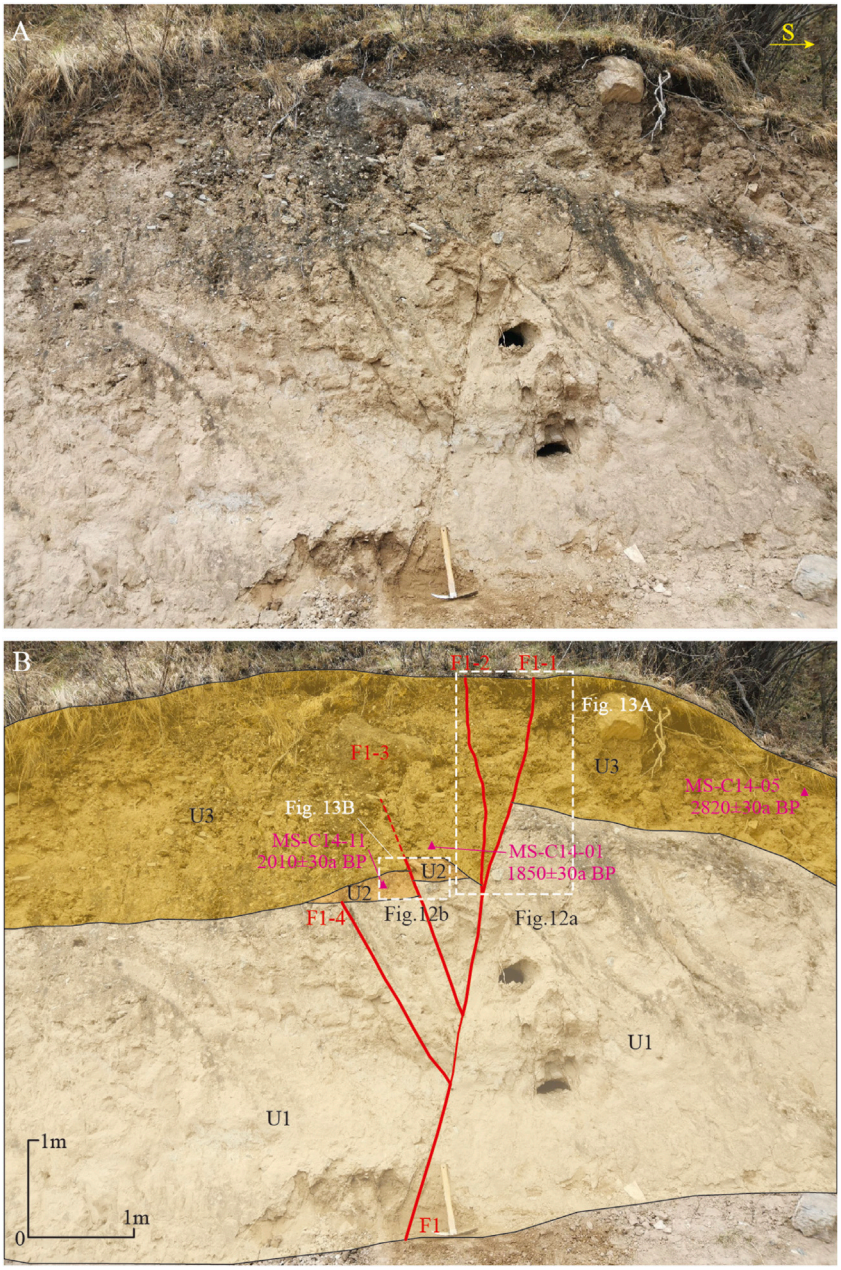

FIGURE 12
Fault outcrop of the Maisu fault near Yongqu, close to Gangtuo (E98.51321°, N31.71495°). According to the dating results of samples collected from the strata dislocated by the fault, the Maisu fault is a Holocene-active fault. **(A)** Photograph showing the fault outcrop. **(B)** Interpretation of the fault outcrop and the locations of the dating samples.

4.6 The yongqu site

We identified another fault exposure at the Yongqu site. Cleaning the outcrop revealed a very obvious upward-branching fault that cuts across the Quaternary stratum. Three stratigraphic units were revealed, labeled U1–U3 from bottom to top (Figures 12, 13). Unit U1 is composed of yellow silt–fine sand and contains some gravels. The lower part of Unit U2 is composed of small gravel with poor roundness. Its upper part is a fine sand layer that pinches out toward the north. Unit U3 is a sand–gravel layer. The gravels in unit U3 are sub-rounded, and their diameters range widely from 5 cm to 20 cm. On the basis of the characteristics of the sedimentary strata and the deformation caused by the fault, we identified two earthquake events. In event I, unit U1 was displaced by the faults, forming a

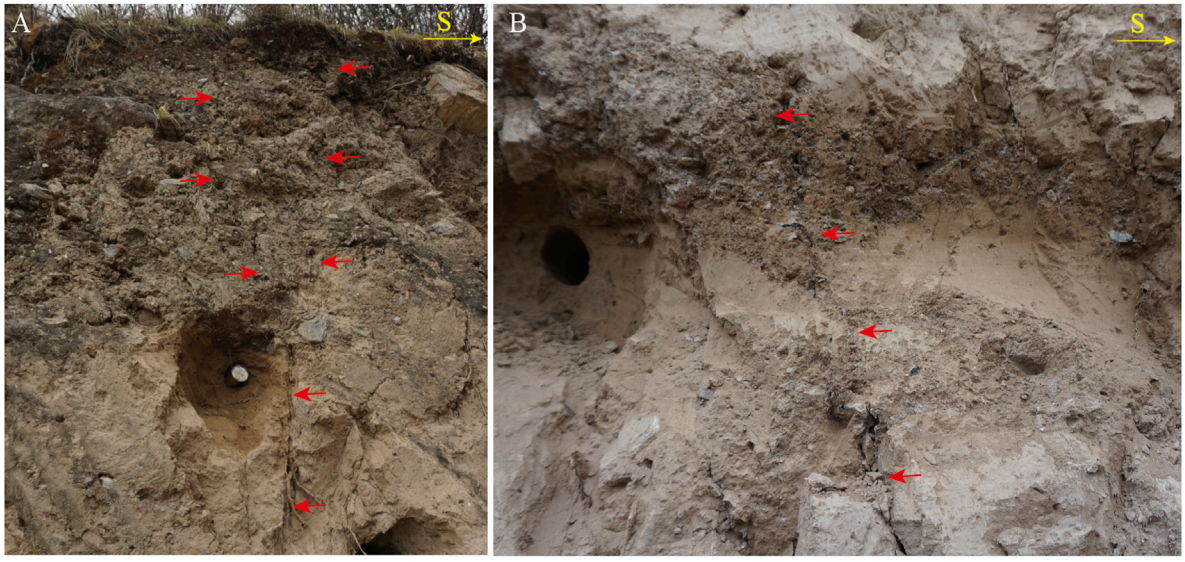

FIGURE 13
Photographs showing partial details of the Maisu fault. **(A)** and **(B)** close-up photographs of the areas defined by the large and small white dashed rectangles, respectively, shown in Figure 12B.

TABLE 1 Radiocarbon ages of the samples collected along the Maisu fault.

Sample	Lab.no	Description	13C/12C (o/oo)	Measured radiocarbon age (a BP)	Conventional radiocarbon age (a BP)
MS-C14-01	607305	Charcoal	−21.7	1800±30	1850±30
MS-C14-05	612636	Charcoal	−23.7	2800±30	2820±30
MS-C14-11	607307	Charcoal	−24.3	2000±30	2010±30

colluvial wedge (U2) and a fault scarp. Unit U3 is thicker on the hanging wall of the fault $F_{1\text{-}1}$ than on the footwall. In event II, the fault displaced all the strata up to the surface. According to the test results of samples MS-C14-01, MS-C14-05, and MS-C14-11, collected from units U2 and U3, event I occurred prior to 2010 ± 30 BP. The test result for MS-C14-05 (2820 ± 30 BP) is older than the actual deposition age of unit U3. The sediments in sample MS-C14-05 may have originated from the erosion of older strata. Therefore, we suggest that event II may have occurred after 1850 ± 30 BP (Table 1).

The raw radiocarbon ages were calibrated by OxCal 4.3.1 (Ramsey and Lee, 2013).

5 Discussion

The Maisu fault is an E–W-tending left-lateral strike-slip fault located in the Sichuan–Yunnan block on the eastern margin of the Tibetan Plateau. The Jinshajiang River and its main tributaries are obviously left-laterally displaced by the fault. At the Worilong site, terrace T3 of the Jinshajiang River has been left-laterally displaced by 21.2 ± 2.0 m. This indicates that the Maisu fault is primarily characterized by left-lateral strike-slip movement. An interpretation of the remote-sensing and field survey data further indicates a earthquake surface rupture zone with a length of 45 km on the fault, which extends from the town of Puma to north of the towns of Babang and Gongya in Dege County, Sichuan Province, finally disappearing near the village of Worilong (near the town of Gangtuo, Xizang Province). The magnitude of the latest strong earthquake calculated using the formulas suggested by Wells and Coppersmith (1994) is approximately Mw 7.

$$\mathrm{Log(SRL)} = 0.74*\mathrm{M} - 3.55 \quad (1)$$

Here, SRL indicates the surface rupture length [km] and M indicates the moment magnitude. According to geological and chronological evidence, the latest earthquake occurred on this fault after 1850 ± 30 BP.

Previously, the Maisu fault was thought to be a late-Pleistocene-active fault (Xu et al., 2016). We estimated the Holocene activity of the Maisu fault based on the geomorphological markers and the radiocarbon dating of the displaced strata. In particular, the latest earthquake on the fault likely occurred after 1850 ± 30 BP with a magnitude of Mw 7. The discovery of Holocene activity along the Maisu fault changes our understanding of the regional kinematics and tectonic deformation. South of the Garzê–Yushu fault, which is the northern boundary fault of the Sichuan–Yunnan block, there are several E–W-trending strike-slip faults with Holocene activity, e.g., the Maisu and Batang faults (the southern boundary fault of the Batang Basin near Yushu County, Qinghai Province), which intersect the Garzê–Yushu fault. Both Huang et al. (2015) and Lü et al. (2017) have suggested that the Batang fault accommodates the partitioned horizontal slip of the Garzê–Yushu fault. The Maisu fault is similar to the Batang fault. It extends eastward and intersects the Garzê–Yushu fault. The intersection of the two faults could lead to partitioning of the horizontal strike-slip, although we have not obtained the horizontal slip rate of the Maisu fault. In addition, there is still no consensus concerning the horizontal slip rate of the southeastern segment of the Garzê–Yushu fault (Zhou et al., 1996, 1997; Wen et al., 2003; Peng et al., 2006; Chevalier et al., 2017). The Maisu fault may also play a role in absorbing the partitioned horizontal slip of the Garzê–Yushu fault.

6 Conclusion

The Maisu fault is one of the numerous E–W-trending strike-slip faults to the south of the Garzê–Yushu fault, which is the northern boundary fault of the Sichuan–Yunnan block. The Maisu fault shows a Holocene activity, and our study identified a well-preserved 45-km-long earthquake surface rupture zone along the fault. The magnitude of the latest major earthquake was estimated to be Mw 7. According to the geological and chronological evidence, this latest major earthquake on the Maisu fault may have occurred after 1850 ± 30 BP.

Data availability statement

The original contributions presented in the study are included in the article/supplementary material, further inquiries can be directed to the corresponding author.

Author contributions

HZ: Field survey, Material and data collection, Writing (original draft); YQ: Field survey, Material and data collection; ML: Conceptualization, Field survey, Material and data collection, Writing (original draft), Writing (review and editing); KS: Field survey, Material and data collection; FH: Field survey, Material and data collection; CL: Field survey, Material and data collection; WZ: Material and data collection; WW: Material and data collection; HZ: Field survey, Conceptualization; YY: Material and data collection.

Funding

The earthquake catalog used for this study was provided by the Sichuan Earthquake Agency, Chengdu, China. This work was financially supported by the National Key Research and Development Program of China (2018YFC1504501-02, 2021YFC3000601), the Lhasa National Geophysical Observation and Research Station (NORSLS21-04), the National Survey on Seismic Disaster Risk Work (10215221024000009001), the State Key Laboratory of Earthquake Dynamics, Institute of Geology, CEA (LED 2020B02), and the Project of Science for Earthquake Resilience (XH21027).

Conflict of interest

The authors declare that the research was conducted in the absence of any commercial or financial relationships that could be construed as a potential conflict of interest.

The reviewer HY declared a shared affiliation with the authors HZ, ML, CL, WZ, WW, KS, FH, HZ to the handling editor at the time of review.

Publisher's note

All claims expressed in this article are solely those of the authors and do not necessarily represent those of their affiliated organizations, or those of the publisher, the editors and the reviewers. Any product that may be evaluated in this article, or claim that may be made by its manufacturer, is not guaranteed or endorsed by the publisher.

References

Chevalier, M. L., Leloup, P. H., Replumaz, A., Pan, J. W., Liu, D. L., Gourbet, L., et al. (2016). Tectonic-geomorphology of the Litang fault system, SE Tibetan Plateau, and implication for regional seismic hazard. *Tectonophysics* 682, 278–292. doi:10.1016/j.tecto.2016.05.039

Chevalier, M. L., Leloup, P. H., Replumaz, A., Pan, J. W., Métois, M., and Li, H. (2017). Temporally constant slip rate along the Ganzi fault, NW Xianshuihe fault system, eastern Tibet. *GSA Bull.* 130, 396–410. doi:10.1130/B31691.1

Deng, Q. D., Cheng, S. P., Ma, J., and Du, P. (2014). Seismic activities and earthquake potential in the Tibetan Plateau. *Chin. J. Geophys.* 57 (07), 2025–2042.

Hou, Z. Q., Hou, L. W., Ye, Q. T., Liu, F. L., and Tang, G. G. (1995). *Yidun island arc structure-magmatic evolution and volcanic massive sulfide deposits in Sanjiang area*. Beijing: Seismological Press, 1–220.

Huang, X. M., Du, Y., He, Z. T., Ma, B. Q., and Xie, F. R. (2015). Late Quaternary slip rate of the Batang Fault and its strain partitioning role in Yushu area, central Tibet. *Tectonophysics* 653, 52–67. doi:10.1016/j.tecto.2015.03.026

Li, Y. B., Wang, H., Liu, H. G., and Chen, L. C. (2016). The surface rupture remains along the Dangjiang segment of Garzê-Yushu fault and the 1738 AD earthquake. *Technol. Earthq. Disaster Prev.* 11 (02), 207–217.

Lin, A. M., Rao, G., Jia, D., Wu, X. J., Yan, B., and Ren, Z. K. (2011). Co-seismic strike-slip surface rupture and displacement produced by the 2010 Mw6.9 Yushu earthquake, China, and implications for Tibetan tectonics. *J. Geodyn.* 52 (3-4), 249–259. doi:10.1016/j.jog.2011.01.001

Lü, L. X. (2017). *Studies on the geometry, kinematics and paleoseismology of the Yushu fault*. China: Institute of Geology, China Earthquake Administration.

Peng, H., Ma, M. X., Bai, J. Q., and Du, D. P. (2006). Characteristics of quaternary activities of the Garzê-Yushu fault zone. *J. Geomechanics* 12 (03), 295–304.

Ramsey, C. B., and Lee, S. (2013). Recent and planned developments of the program oxcal. *Radiocarbon* 55, 720–730. doi:10.1017/s0033822200057878

Wells, D., and Coppersmith, K. (1994). New empirical relationships among magnitude, rupture length, rupture width, rupture area, and surface displacement. *Bull. Seismol. Soc. Am.* 84 (4), 974–1002.

Wen, X. Z., Xu, X. W., Zheng, R. Z., Xie, Y. Q., and Wan, C. (2003). The average sliding rate and recent strong earthquake rupture of the Garzê-Yushu fault. *Sci. China Earth Sci.* 1 (S1), 199–208.

Wen, X. Z., Zhang, P. Z., Du, F., and Long, F. (2009). The back ground of historical and modern seismic activities of the occurrence of the 2008 MS8.0 Wenchuan, Sichuan, earthquake. *Chin. J. Geophys* 52 (2), 444–454.

Wu, F. R., Jiang, L. W., Zhang, G. Z., and Wang, D. (2019). Discussion on quaternary activity characteristics of northern section of Jinshajiang fault along Sichuan-Tibet railway. *High. Speed Railw. Technol.* 10 (04), 23–28+43.

Wu, T., Xiao, L., Gao, R., Yang, H. J., and Yang, G. (2014). Petrogenesis and tectonic setting of the Queershan composite granitic pluton, Eastern Tibetan Plateau: Constraints from geochronology, geochemistry and Hf isotope data. *Sci. China Earth Sci.* 44 (08), 2712–2725. doi:10.1007/s11430-014-4936-y

Xia, J. W., and Zhu, M. (2020). Study on tectonic characteristics and activity of middle section of Jinshajiang Main Fault Zone. *Yangtze River* 51 (5), 131–137.

Xu, X. W., Han, Z. J., Yang, X. P., Zhang, S. M., Yu, G. H., Zhou, B. G., et al. (2016). *Seismic tectonic map of China and neighboring areas*. Beijing: Seismological Press.

Xu, X. W., Wen, X. Z., Ye, J. Q., Ma, B. Q., Chen, J., Zhou, R. J., et al. (2008). The Ms8.0 wenchuan earthquake surface ruptures and its seismogenic structure. *Seismol. Geol.* 30 (3), 597–629.

Xu, X. W., Wen, X. Z., Zheng, R. Z., Ma, W. T., Song, F. M., and Yu, G. H. (2003). The latest tectonic change pattern and power source of active blocks in the Sichuan-Yunnan region. *Sci. China Earth Sci.* 46 (S1), 151–162.

Xu, X. W., Zhang, P. Z., Wen, X. Z., Qin, Z. L., Chen, G. H., and Zhu, A. L. (2005). Features of active tectonics and recurrence behaviors of strong earthquakes in the Western Sichuan province and its adjacent rejoins. *Seismol. Geol.* 27 (03), 446–461.

Xu, Z. Q., Hou, L. W., Wang, Z. X., Fu, X. F., and Huang, M. H. (1992). *The orogenic process of the Songpan- Garzê orogenic belt in China*. Beijing: Geology Press.

Yi, G. X., Long, F., Liang, M. J., Zhang, H. P., Zhao, M., Ye, Y. Q., et al. (2017). Focal mechanism solutions and seismogenic structure of the 8 August, 2017 M7.0 Jiuzhaigou earthquake and its aftershocks, northern Sichuan. *Chin. J. Geophys.* 60 (10), 4083–4097.

Yuan, D. Y., Feng, J. G., Zheng, W. J., Liu, X. W., Ge, W. P., and Wang, W. T. (2020). Migration of large earthquakes in Tibetan block area and discussion on major active region in the future. *Seismol. Geol.* 42 (02), 297–315.

Zeng, Q., and Xu, T. D. (2019). An approach to the Neogene uplift rates for the eastern Qinghai-Xizang Plateau: Evidence from the fission track ages of the apatite from the Chola granites in Western Sichuan. *Sediment. Geol. Tethyan Geol.* 39 (03), 92–100.

Zhao, H., Li, D. H., Zhao, J., Zhang, L., and Chen, X. F. (2021). Exploration for the southern segment of the Garzê-Yushu fault zone using shallow seismic reflection method. *Earthq. Res. Sichuan* 1 (01), 6–11. doi:10.13716/j.cnki.1001-8115.2021.01.002

Zhou, C. J., Wu, Z. H., Nima, C. R., Li, J. C., Jiang, Y., and Liu, Y. H. (2014). Structural analysis of the co-seismic surface ruptures associated with the Yushu Ms7.1 earthquake, Qinghai Province. *Geol. Bull. China* 33 (4), 551–566.

Zhou, R. J., Chen, G. X., Li, Y., Zhou, C. H., Gong, Y., He, Y. L., et al. (2005). Research on active faults in Litang-Batang region, Western Sichuan province, and the seismogenic structures of the 1989 Batang M6.7 earthquake swarm. *Seismol. Geol.* 1 (01), 31–43.

Zhou, R. J., Ma, H. S., and Cai, C. X. (1996). Late quaternary active features of the Garzê-Yushu fault zone. *Earthq. Res. China* 1 (03), 250–260.

Zhou, R. J., Wen, X. Z., Cai, C. X., and Ma, S. H. (1997). Recent earthquakes and assessment of seismic tendency on the Garzê-Yushu fault zone. *Seismol. Geol.* 1 (02), 20–29.